

## MIT Open Access Articles

*Simulated Response of the Arctic Freshwater  
Budget to Extreme NAO Wind Forcing*

The MIT Faculty has made this article openly available. **Please share**  
how this access benefits you. Your story matters.

**Citation:** Condron, Alan et al. "Simulated Response of the Arctic Freshwater Budget to Extreme NAO Wind Forcing." *Journal of Climate* (2009): 2422-2437. © 2008 American Meteorological Society

**As Published:** <http://dx.doi.org/10.1175/2008JCLI2626.1>

**Publisher:** American Meteorological Society

**Persistent URL:** <http://hdl.handle.net/1721.1/52327>

**Version:** Final published version: final published article, as it appeared in a journal, conference proceedings, or other formally published context

**Terms of Use:** Article is made available in accordance with the publisher's policy and may be subject to US copyright law. Please refer to the publisher's site for terms of use.



# Simulated Response of the Arctic Freshwater Budget to Extreme NAO Wind Forcing

ALAN CONDRON

*Department of Earth, Atmospheric and Planetary Sciences, Massachusetts Institute of Technology,  
Cambridge, Massachusetts*

PETER WINSOR

*School of Fisheries and Marine Sciences, University of Alaska Fairbanks, Fairbanks, Alaska*

CHRIS HILL

*Department of Earth, Atmospheric and Planetary Sciences, Massachusetts Institute of Technology,  
Cambridge, Massachusetts*

DIMITRIS MENEMENLIS

*Jet Propulsion Laboratory, California Institute of Technology, Pasadena, California*

(Manuscript received 13 May 2008, in final form 7 November 2008)

## ABSTRACT

The authors investigate the response of the Arctic Ocean freshwater budget to changes in the North Atlantic Oscillation (NAO) using a regional-ocean configuration of the Massachusetts Institute of Technology GCM (MITgcm) and carry out several different 10-yr and 30-yr integrations. At  $1/6^\circ$  ( $\sim 18$  km) resolution the model resolves the major Arctic transport pathways, including Bering Strait and the Canadian Archipelago. Two main calculations are performed by repeating the wind fields of two contrasting NAO years in each run for the extreme negative and positive NAO phases of 1969 and 1989, respectively. These calculations are compared both with a control run and the compiled observationally based freshwater budget estimate of Serreze et al.

The results show a clear response in the Arctic freshwater budget to NAO forcing, that is, repeat NAO negative wind forcing results in virtually all freshwater being retained in the Arctic, with the bulk of the freshwater content being pooled in the Beaufort gyre. In contrast, repeat NAO positive forcing accelerates the export of freshwater out of the Arctic to the North Atlantic, primarily via Fram Strait ( $\sim 900 \text{ km}^3 \text{ yr}^{-1}$ ) and the Canadian Archipelago ( $\sim 500 \text{ km}^3 \text{ yr}^{-1}$ ), with a total loss in freshwater storage of  $\sim 13\,000 \text{ km}^3$  (15%) after 10 yr. The large increase in freshwater export through the Canadian Archipelago highlights the important role that this gateway plays in redistributing the freshwater of the Arctic to subpolar seas, by providing a direct pathway from the Arctic basin to the Labrador Sea, Gulf Stream system, and Atlantic Ocean.

The authors discuss the sensitivity of the Arctic Ocean to long-term fixed extreme NAO states and show that the freshwater content of the Arctic is able to be restored to initial values from a depleted freshwater state after  $\sim 20$  yr.

## 1. Introduction

The stability and response of the meridional overturning circulation (MOC) to identical freshwater perturbation and emission scenarios varies greatly between

different models (e.g., Manabe and Stouffer 1988; Rahmstorf 1995; Stouffer et al. 2006). One of the main factors controlling the strength and sensitivity of the MOC is the representation of the freshwater budget of the high latitudes. In the open-ocean deep convection regions of the North Atlantic a delicate density balance exists so that only slight variations in Arctic–North Atlantic freshwater exchanges have an effect on the strength of the overturning cell by interrupting the formation of North Atlantic Deep Water (NADW) (Aagaard and

---

*Corresponding author address:* Dr. Alan Condron, Department of Earth, Atmospheric and Planetary Sciences, Massachusetts Institute of Technology, Cambridge, MA 02139.  
E-mail: acondron@whoi.edu

Carmack 1989; Mysak et al. 2005; Rahmstorf et al. 2005; Zhang and Vallis 2006). In recognition of the importance of understanding the impact of freshwater exchanges between the Arctic and the Atlantic, the Arctic/Subarctic Ocean Fluxes (ASOF) program was set up in 1999 with the aim of measuring and improving the modeling of these fluxes.

A change in the Arctic freshwater budget between 1965 and 1995 is believed to have increased the export of freshwater to the North Atlantic, as observed by a freshening of the North Atlantic by an amount equivalent to  $\sim 19\,000 \pm 5000 \text{ km}^3$  [ $31\,536 \text{ km}^3 \text{ yr}^{-1} = 1 \text{ Sv}$  ( $\text{Sv} \equiv 10^6 \text{ m}^3 \text{ s}^{-1}$ )] of freshwater (Curry and Mauritzen 2005; Peterson et al. 2006). About half of this freshwater appears to have been released from the Arctic during the Great Salinity Anomaly (GSA), which began in 1968, when increased ice export in Fram Strait discharged  $\sim 2000 \text{ km}^3 \text{ yr}^{-1}$  of freshwater into the northern North Atlantic over a 5-yr period (Dickson et al. 1988). Similar GSAs occurred in the 1980s and 1990s (Belkin et al. 1998; Belkin 2004), and all appear to have their origin in the Arctic (Haak et al. 2003; Sundby and Drinkwater 2007). Observations of the 1960s GSA indicate that the additional freshwater added to the Labrador Sea inhibited the production of Labrador Seawater (LSW) (Lazier 1980), while modeling studies of this event have shown that the reduced LSW formation may have, in fact, weakened the strength of the MOC by 1–3 Sv (Mysak et al. 2005; Zhang and Vallis 2006). Considering this rather large change in the MOC, we note that an additional annual release of only 2% of the freshwater stored in the Arctic over a 5-yr period would generate a signal comparable to that of the GSA.

The changes outlined have been paralleled with changes in the water mass structure and properties of the Arctic Ocean (Quadfasel et al. 1991; Steele and Boyd 1998; Morison et al. 2000). Atlantic Water (AW) entering the Arctic via the Barents shelf and West Spitzbergen Current (WSP) have warmed since the early 1990s, producing temperature anomalies in the Nansen Basin of roughly  $+1^\circ\text{C}$  in 2004 (Polyakov et al. 2005). The increased penetration of AW caused the cold halocline (CHL) to retreat from the Amundsen Basin to the Makarov Basin in the mid-1990s (Steele and Boyd 1998), although measurements showed that it had returned to the Amundsen Basin in 2001 (Björk et al. 2002).

Large-scale interannual changes in the atmospheric circulation over the Arctic appear to have played a dominant role in the observed changes in the freshwater budget and water mass structure of the Arctic Ocean (Morison et al. 2000; Häkkinen and Proshutinsky 2004; Karcher et al. 2005; Peterson et al. 2006; Köberle and Gerdes 2007). The atmospheric circulation of the Arctic

is dominated by the North Atlantic Oscillation (NAO)/Arctic Oscillation (AO) (Hurrell 1995; Thompson and Wallace 1998), which switched from its most extreme negative state in the 1960s to its most extreme prolonged positive state in the early 1990s (Fig. 1a).<sup>1</sup> Häkkinen and Proshutinsky (2004) and Köberle and Gerdes (2007) both simulated the Arctic freshwater budget from the 1950s to the early 2000s using two different coupled ocean–ice regional Arctic models, forced with atmospheric National Centers for Environmental Prediction–National Center for Atmospheric Research (NCEP–NCAR) reanalysis data (Kalnay et al. 1996). Both models show a reduction in the freshwater content of the Arctic by  $\sim 5000 \text{ km}^3$  between the 1980s and the mid-1990s, followed by an increase of similar magnitude by the early 2000s. The change in freshwater storage occurs in parallel with the weakening of the NAO from its persistent high state in the early 1990s, toward a more neutral state after the mid-1990s.

The direct response of the Arctic freshwater budget to the positive and negative phases of the NAO pattern were recently examined by Zhang et al. (2003), and then by Houssais et al. (2007), using regional coupled ocean–ice models of the Arctic, forced with NCEP data. To create atmospheric forcing fields for the NAO, the NCEP data were regressed onto the positive and negative phases of the NAO index over the last 50 years. Interestingly, even though both authors used different models, their findings are quite similar. We note, however, that Houssais et al. primarily focused on the response of the Arctic to positive NAO forcing. During the positive NAO forcing, the freshwater storage in the Arctic is reduced due to an increase in the export of sea ice and liquid freshwater in Fram Strait and the Canadian Archipelago.

It is hypothesized that the response of the freshwater budget to the NAO is caused by a switch from anticyclonic to cyclonic atmospheric circulation over the central Arctic (Häkkinen and Proshutinsky 2004). During the negative phase of the NAO, the strong Beaufort high pressure (Fig. 1b) results in an anticyclonic atmospheric circulation over the central Arctic, causing freshwater to be stored/retained in the Beaufort gyre, owing to Ekman convergence. In contrast, during the positive phase of the NAO, the Beaufort high weakens and is replaced by a cyclonic circulation (Fig. 1c). This pattern is associated with an intensification of the North

<sup>1</sup> We note that the NAO and the AO are nearly indistinguishable, with a monthly temporal correlation of 0.95 Deser (2000), so we focus on the NAO index based on the difference of normalized winter (December–March) sea level pressure between Lisbon, Portugal, and Stykkisholmur/Reykjavik, Iceland (Hurrell 1995).

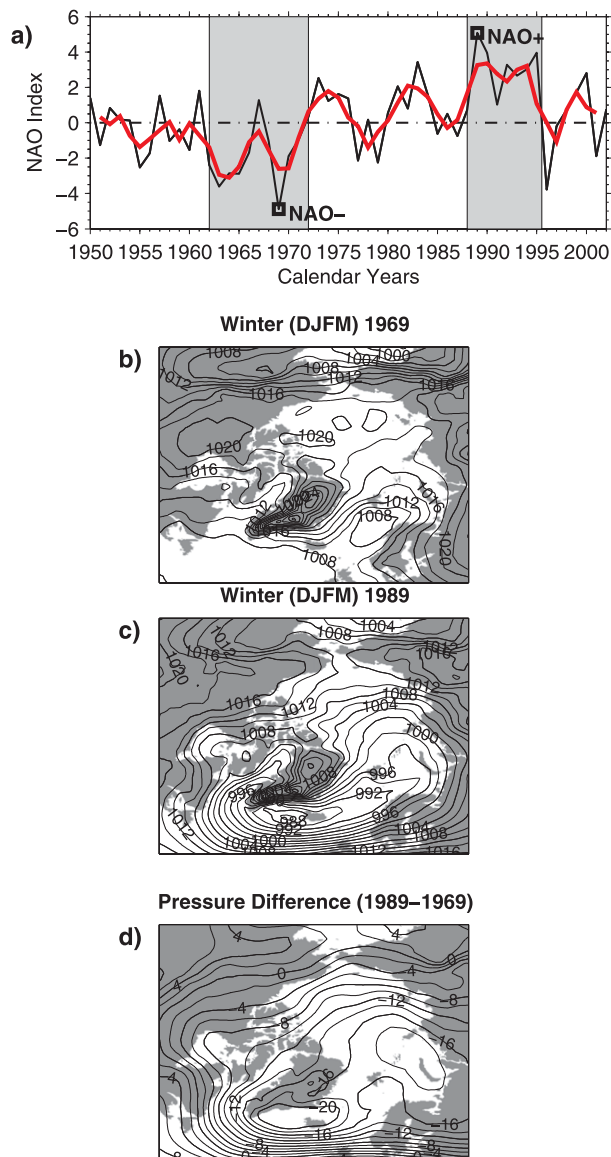


FIG. 1. (a) The winter [December–March (DJFM)] NAO index from Hurrell (1995; updated and available online at <http://www.cgd.ucar.edu/cas/jhurrell/indices.html>). The 5-yr running mean is plotted (red), and the extreme NAO negative and positive years of 1969 and 1989, respectively, are marked (black squares). The persistence of the NAO in its negative and positive phase for close to a decade in the 1960s and 1990s, respectively, is highlighted (gray shading). Winter (DJFM) mean sea level pressure (hPa) from NCEP reanalysis for the (b) NAO negative year 1969 (NAO-) and (c) NAO positive year 1989 (NAO+). Note the anticyclonic high pressure over the Arctic in 1969, in contrast to the cyclonic circulation in 1989. (d) The difference in pressure between 1969 and 1989 (NAO+ minus NAO-). The contour interval in all pressure maps is 2 hPa.

Atlantic storm track and an increased northward atmospheric heat transport. The reduced Ekman convergence can no longer retain the freshwater in the Beaufort gyre, causing it to be exported into the North Atlantic (Proshutinsky et al. 2002; Zhang et al. 2003; Häkkinen and Proshutinsky 2004; Peterson et al. 2006). At the same time, an intensified sea level pressure gradient in Fram Strait drives sea ice into the North Atlantic (Kwok et al. 2004).

The main focus of this paper is to investigate changes in the Arctic freshwater budget, and the storage and release of freshwater to the North Atlantic Ocean, in response to the wind forcing during the positive and negative phases of the NAO. Despite previous work, the different response of the Arctic freshwater budget—in terms of storage, release, and exchange with the North Atlantic to the negative and positive phases of the NAO—continues to remain unclear. We note that many modeling studies of the Arctic freshwater budget discussed previously suffered from two shortcomings that likely lead to inaccuracies. First, and most importantly, previous model studies restore salinity and/or temperature to climatological values to avoid model drift (Zhang et al. 1998b; Maslowski et al. 2000; Zhang et al. 2003; Karcher et al. 2005). The strength of the restoring typically varies from days to months in these simulations, but any restoring makes deriving an accurate freshwater budget of the Arctic difficult. Second, we note that the resolution of the regional models (typically  $1^\circ$ ) used to examine the freshwater budget requires a simplification of the exchange with the northwest Atlantic through the complex network of channels in the Canadian Archipelago. This is typically done by either prescribing the flow using climatological values or by simplifying the region to one or two large straits (Zhang et al. 1998b; Maslowski et al. 2000; Karcher et al. 2005).

We begin this paper with a brief description of the model and its setup (section 2) and then evaluate the performance of the model in the Arctic by comparing it to an observed climatological Arctic freshwater budget (section 3). The response of the Arctic freshwater budget to changes in the NAO is then determined by forcing the model with two extreme positive and negative phases of this oscillation (section 4). Conclusions are then drawn (section 5).

## 2. Model description and calculations

### a. Model description

The numerical calculations presented here employ a coupled ocean sea ice configuration of the MIT general circulation model (MITgcm) (Marshall et al. 1997). The

MITgcm configuration used covers a limited-area Arctic domain that has open boundaries at  $\sim 55^\circ$  in the Atlantic and Pacific sectors. The exact boundary lines coincide with grid cells in a global cubic sphere MITgcm configuration (Menemenlis et al. 2005; Fig. 2). This global configuration is used to provide monthly boundary conditions of potential temperature, salinity, flow, and sea surface elevation to the simulations presented in this paper.

The grid covering the Arctic domain is locally orthogonal and has a variable horizontal resolution with an average spacing of  $\sim 18$  km. Although this grid spacing is not eddy resolving (deformation radius in the Arctic is  $\sim 5$ – $10$  km), the mesh resolves major Arctic straits, including many of the channels of the Canadian Archipelago. The sea ice and ocean equations are solved on the same horizontal mesh. The height-based vertical gridding option of MITgcm is utilized with 50 vertical levels and spacing set to vary from  $\sim 10$  m near the surface to  $\sim 450$  m at a depth of  $\sim 6000$  m. The vertical resolution is greatest in the upper ocean with 20 vertical levels in the top 300 m, which permit a good representation of freshwater in the Arctic halocline. Bathymetry is derived from the U.S. National Geophysical Data Center (NGDC) 2' global relief dataset (ETOPO2), which uses the International Bathymetric Chart of the Arctic Ocean (IBCAO) product for Arctic bathymetry. The ETOPO2 data is smoothed to the model horizontal mesh and mapped to the ocean vertical levels using a "lopped cell" strategy (Adcroft et al. 1997) that permits an accurate representation of the ocean bottom boundary.

Initial ocean hydrography is taken from the Polar Science Center Hydrographic Climatology (PHC) 3.0 database (Steele et al. 2001). The initial sea ice distribution is from the Pan-Arctic Ice–Ocean Modeling and Assimilation System (PIOMAS) datasets (Zhang and Rothrock 2003). Atmospheric state (10-m surface wind, 2-m air temperature and humidity, and downward longwave and shortwave radiation) is taken from the 6-hourly NCEP–NCAR reanalysis (Kalnay et al. 1996). Monthly mean estuarine fluxes of freshwater are based on the Regional, Electronic, Hydrographic Data Network for the Arctic Region (R-ArcticNET) dataset (Lammers et al. 2001).

The ocean component is configured to use an equation of state formulated according to Jackett and McDougall (1995). Ocean surface fluxes (in the absence of sea ice) are calculated using the bulk formula of Large and Pond (1981). Boundary layer and convective mixing in the ocean is parameterized according to Large et al. (1994). Background vertical diffusivity of temperature and salinity are set to  $4 \times 10^{-6} \text{ m}^2 \text{ s}^{-1}$ , and an enhanced

vertical diffusivity of  $1 \times 10^{-4} \text{ m}^2 \text{ s}^{-1}$  is active at depth, motivated by Bryan and Lewis (1979). Tracer transport equations are solved using a high-order monotonicity-preserving scheme (Daru and Tenaud 2004). Nonlinear momentum terms are solved using a vector invariant formulation (Adcroft et al. 2004) with viscous dissipation following Leith (1969), but modified to dissipate divergence as well as vorticity. In our model configuration, the parameterization of geostrophic eddies using the method of Gent–McWilliams (GM)/Redi (Redi 1982; Gent and McWilliams 1990) was disabled. Furthermore, there is no overflow parameterization.

The sea ice component of the system follows the viscous–plastic rheology formulation of Hibler (1979), with momentum equations solved implicitly on a C grid (Arakawa 1977) using a procedure based on Zhang and Hibler (1997). The initial sea ice field is taken from the PIOMAS dataset. The data are available freely online ([http://psc.apl.washington.edu/IDAO/data\\_piomas.html](http://psc.apl.washington.edu/IDAO/data_piomas.html)), and are described by Zhang and Rothrock (2003). Fluxes of momentum into ice due to the overlying atmospheric winds and momentum fluxes between sea ice and the ocean are calculated by solving for the momentum balance at each surface grid column (Hibler and Bryan 1987). The ocean–sea ice coupled system is stepped forward synchronously with a time step of 1800 s.

Freezing and melting of sea ice and associated fluxes of heat and freshwater between the ocean, sea ice, and atmosphere are calculated by solving a heat balance equation for each surface grid column at each time step (Zhang et al. 1998a; Parkinson and Washington 1979; Semtner 1976). When air temperatures are below freezing, precipitation falls as snow. Snow falling on the sea ice is advected with the ice movement, and will gradually be transformed into sea ice as it accumulates. Sea ice is assumed to be entirely fresh and have a density of  $920 \text{ kg m}^{-3}$ , while the density of snow is fixed at  $330 \text{ kg m}^{-3}$ .

It is important to note that there is no salinity or temperature restoring in the model—allowing us to more accurately model the Arctic freshwater budget.

### *b. Model calculations*

We performed a control run by forcing the model with 6-hourly NCEP reanalysis data for 10 years from January 1992 to December 2001. To understand the response of the Arctic to the different states of the NAO we then reran the model from rest, keeping all reanalysis fields exactly the same as the control simulation, except that we repeatedly cycled the 6-hourly wind field for two contrasting NAO years in each integration for 10 years. We note that due to the tendency for the NAO to persist in one phase on a decadal scale (as highlighted

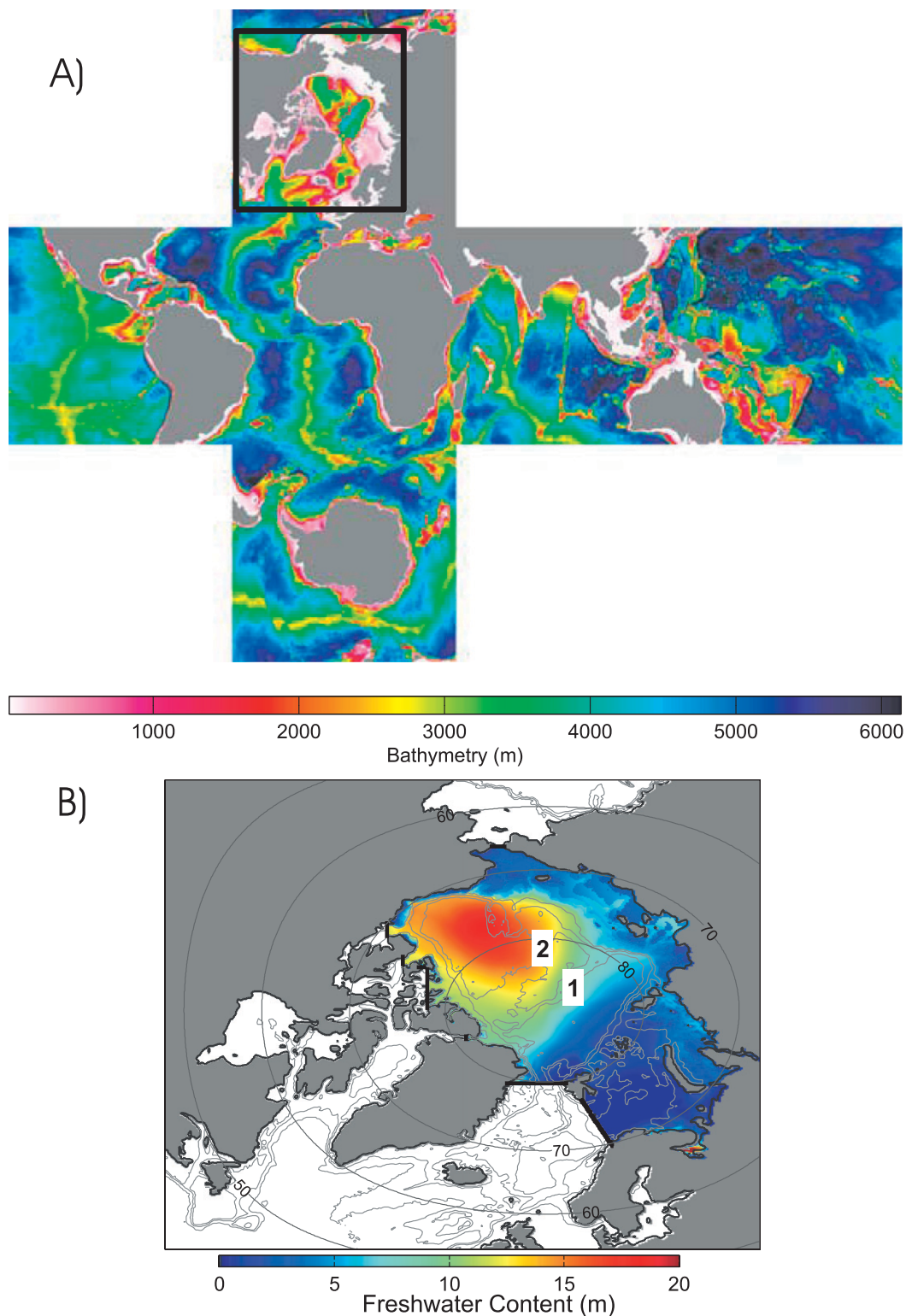


FIG. 2. (a) Bathymetry of the global cubed-sphere ocean model configuration from which our regional model is carved and used to provide open boundary conditions. (b) The regional model presented in this study is a slightly smaller domain than the global Arctic cubed-sphere grid shown in Fig. 2a. Open boundary conditions are taken from the global model integration. The location of the straits used to determine the freshwater budget of the Arctic (thick black lines). The colored region (showing the freshwater content of the Arctic) is synonymous with the Arctic.

in Fig. 1a), a 10-yr integration of the model in each phase seems appropriate. The decadal periodicity of the NAO has previously been commented upon by several authors, including Dickson et al. (2000) when discussing the Arctic's response to the NAO; Hurrell (1995) examining the decadal nature of the NAO; and Proshutinsky and Johnson (1997) studying approximately decadal length (cyclonic and anticyclonic) wind regimes in the Arctic, since the 1960s. Further justification for keeping the NAO in the same phase for this length of time comes from Stephenson et al. (2006) who observed that the NAO index remained positive during the twenty-first century in a significant number of climate prediction runs under rising levels of atmospheric carbon dioxide. It thus appears that as the climate warms the NAO index may favor a positive state for periods longer than a decade.

We use the 6-hourly wind velocity data from the two most extreme negative and positive NAO years in the instrumental record of 1969 and 1989, respectively (Fig. 1a). We note that by only adjusting the wind field and allowing all other forcings, such as 2-m air temperature, humidity, precipitation, etc., to vary with time, we can more easily diagnose the response in the model to a known perturbation. Furthermore, an analysis of the difference between precipitation for years when the NAO was one standard deviation greater (NAO+) or less (NAO-) than the mean for the period 1948–2002 indicates that precipitation rates varied by only  $38.4 \text{ km}^3 \text{ yr}^{-1}$  between the two phases of the NAO. This change is less than 1.5% of the annual rate of precipitation in the control integration, is at least two orders of magnitude less than the major freshwater sources and sinks to the Arctic, and would therefore have a small impact on the overall freshwater budget of the Arctic.

The mean sea level pressure maps show the very different atmospheric circulation patterns in the Arctic for these two years. During the NAO negative year of 1969 (hereafter NAO-), the Beaufort high pressure is evident over the western Arctic, with a mean sea level pressure of 1020 hPa, resulting in an anticyclonic circulation pattern. In contrast, the NAO positive year of 1989 (hereafter NAO+) shows an intensified Icelandic low pressure and a cyclonic circulation pattern persisting over the Arctic Ocean. In summer (not shown) the Beaufort high is replaced by low pressure, giving a cyclonic circulation pattern. We therefore note that for

NAO+ years the atmospheric circulation remained largely cyclonic for the entire year.

To visualize the export pathways of the stored freshwater from the Arctic to the North Atlantic, we add a passive dye to the Arctic in the upper 200 m everywhere the vertical thickness of freshwater exceeds 16 m. In addition, to get a first-order understanding about the system's response we performed a 30-yr-long NAO+ integration, and a 20-yr NAO- integration that starts from the conditions in the Arctic after 10 years of NAO+ forcing. During these experiments, both the 6-hourly NCEP data (excluding wind) and the monthly open boundary conditions, for the period from 1992 to the end of 2001, are cycled three times.

### 3. The Arctic freshwater budget

A minimum requirement for using a model to understand the response of the Arctic to the different phases of the NAO is the ability to represent the present-day Arctic freshwater budget. We derive a freshwater budget for the model Arctic, based on the annual average of the 10-yr control integration, and compare its freshwater storage and release and exchanges with adjacent oceans to the observational Arctic freshwater budget of Serreze et al. (2006). This observed freshwater budget offers an improvement over the original Arctic Ocean freshwater budget produced by Aagaard and Carmack (1989) by synthesizing large amounts of observational data gathered over the 1990s. For historic reasons, the storage and fluxes of freshwater are calculated to a reference salinity of 34.8 psu—a value that approximates the average salinity of the Arctic Ocean (Aagaard and Carmack 1989).

Serreze et al. (2006) estimate the total liquid freshwater storage of the Arctic to be  $74\,000 \text{ km}^3$  ( $\pm 10\%$ ), with  $\sim 60\%$  of this freshwater stored in the central Beaufort Sea, using the same PHC salinity dataset that we used to initialize our model. The large storage of freshwater in this region is visible by a  $\sim 20\text{-m}$  maximum thickness of freshwater when freshwater content is vertically integrated from the surface to the bottom (Fig. 2b). The freshwater content (m) is given by

$$\text{FW}_{\text{storage}} = \int_{\text{Depth}}^0 \left(1 - \frac{S}{S_{\text{ref}}}\right) dz, \quad (1)$$

where  $S$  is salinity,  $S_{\text{ref}}$  the reference salinity of 34.8 psu, and  $dz$  the vertical cell thickness of the dataset. Water

←

FIG. 2. (Continued) domain of Serreze et al. (2006), and is the Arctic domain used for all modeled freshwater budget calculations. Bathymetry contours are drawn at 200 m, 1000 m, and 2500 m; “1” and “2” correspond to the location of the Lomonosov and Mendeleev Ridges, respectively. Colors show the vertically integrated freshwater content, calculated from the PHC database (see text for details).

that has a salinity value higher than 34.8 psu is considered salty, and therefore is not included in this calculation. The sea ice component of freshwater storage is estimated to be  $\sim 10\,000\text{ km}^3$ . It is based on the mean annual extent of sea ice from satellite passive microwave observations over the period 1979–2001, multiplied by an ice thickness of 2.0 m and converted to freshwater assuming the density of ice to be  $900\text{ kg m}^{-3}$  (Serreze et al. 2006). As noted by the authors, sparse information on sea ice thickness leads to large uncertainties in this estimate of freshwater storage. Taken together, the total freshwater storage of the Arctic is estimated to be  $\sim 84\,000\text{ km}^3$ .

In this study we define an Arctic region that is the same as the domain used by Serreze et al. (2006). This Arctic region is the area north of Fram Strait, the Barents Sea, Bering Strait, and the Canadian Archipelago, and corresponds to the color-shaded region in Fig. 2b. Interpolating the PHC data onto the model grid gives an initial liquid freshwater content of  $65\,682\text{ km}^3$ , despite using a very similar Arctic domain to Serreze et al. This reduction in freshwater content, compared to the climatological value of  $74\,000\text{ km}^3$ , is an artifact of our interpolation scheme; by masking the original  $1^\circ \times 1^\circ$  PHC data to our Arctic domain, we obtain a total freshwater content of  $76\,664\text{ km}^3$ : a value only  $2664\text{ km}^3$  different from the estimate of Serreze et al.

The 10-yr annual-mean liquid freshwater content in the model is  $64\,779\text{ km}^3$  and reveals interannual variability in storage and release balanced by changes in freshwater exchanges. The initial PIOMAS sea ice climatology gives a freshwater content of  $21\,912\text{ km}^3$ , assuming a sea ice density of  $920\text{ kg m}^{-3}$ , which over the 10-yr control run averages  $18\,353\text{ km}^3$ . Summing the 10-yr average liquid and sea ice freshwater volumes gives a total freshwater volume of  $83\,131\text{ km}^3$  (Fig. 3): a value in very good agreement with the  $84\,000\text{ km}^3$  reported by Serreze et al.).

The Arctic Ocean exchanges freshwater with the North Atlantic via Fram Strait, the Barents Sea, and the Canadian Archipelago. Freshwater from the Pacific Ocean enters the Arctic through Bering Strait, allowing a high-latitude exchange between the North Pacific and North Atlantic Oceans. To determine the flux of freshwater in each of these regions we consider salinities less than the reference salinity 34.8 psu to be freshwater sources to the Arctic, and fluxes with salinities greater than 34.8 psu to be freshwater sinks. In the model, a series of gates are placed at each pathway (see Fig. 2b) to allow the freshwater transport to be calculated:

$$\text{FW}_{\text{FLUX}} = \int_L dl \int_{\text{Depth}}^0 \left(1 - \frac{S}{S_{\text{ref}}}\right) U_n dz, \quad (2)$$

where  $L$  is the length of the section,  $U_n$  the ocean velocity normal to the vertical section, and  $dl$  the cell width.

The fluxes of freshwater (liquid and ice) through the four pathways in the climatology and the model are shown in Table 1 and Fig. 3. The climatological values are based upon the best estimate of each flux from a large number of different sources, and are discussed in detail in Serreze et al. (2006). Freshwater sources to the Arctic in the climatology are from precipitation (37%), river runoff (28%), and laterally through Bering Strait (35%). Freshwater sinks to the Arctic comprise of evaporation (10%), lateral flow through Fram Strait (56%), the Barents Sea (10%), and through the Canadian Archipelago (24%).

Continental discharge to the Arctic is dominated by four major river systems (the Ob, Yenisey, and Lena in Eurasia and the Mackenzie in Canada) that peak during the spring melt. Instrumental records estimate the total mean annual discharge to be  $2500\text{ km}^3$ , although this value is believed to be an underestimation owing to unaccounted discharge from ungauged rivers. When corrected, an annual discharge of  $3200\text{ km}^3$  is obtained. We note that the annual mean river runoff of  $2009\text{ km}^3\text{ yr}^{-1}$  that we apply to the model is therefore too low compared to observations—a result of not correcting for ungauged river flow.

Climatological values of precipitation ( $P$ ) are taken from a network of gauges in the Arctic, with an annual mean of  $3300\text{ km}^3$ . Evaporation ( $E$ ) over the Arctic acts to increase the ocean salinity, giving a  $P - E$  value of  $2000\text{ km}^3\text{ yr}^{-1}$ . In the model, evaporation is calculated as a function of latent heat of vaporization, which is dependant on the bulk aerodynamic flux formula and model sea surface temperature. Considering this, the model  $P - E$  value of  $1969\text{ km}^3\text{ yr}^{-1}$  is in good agreement with the climatology. Note that this value, and all subsequent values reported for the model, is the 10-yr mean from the model simulation.

The lateral inflow of liquid freshwater from Bering Strait represents the only major oceanic freshwater source into the Arctic. Climatology values of  $2500\text{ km}^3\text{ yr}^{-1}$  are in close agreement with the model value of  $2465\text{ km}^3\text{ yr}^{-1}$ . We find in our model that there is a  $52\text{ km}^3\text{ yr}^{-1}$  inflow of sea ice into the Chukchi Sea region through Bering Strait, although no value is given for this flux in the climatology (Serreze et al. 2006).

At Fram Strait, warm salty Atlantic Water (AW) enters the Arctic through the eastern part of the strait as the West Spitzbergen Current, while a return flow of cold, fresh Arctic water and sea ice takes place to the west, in the East Greenland Current (EGC). The respective directions of these flows ensure that both currents act as

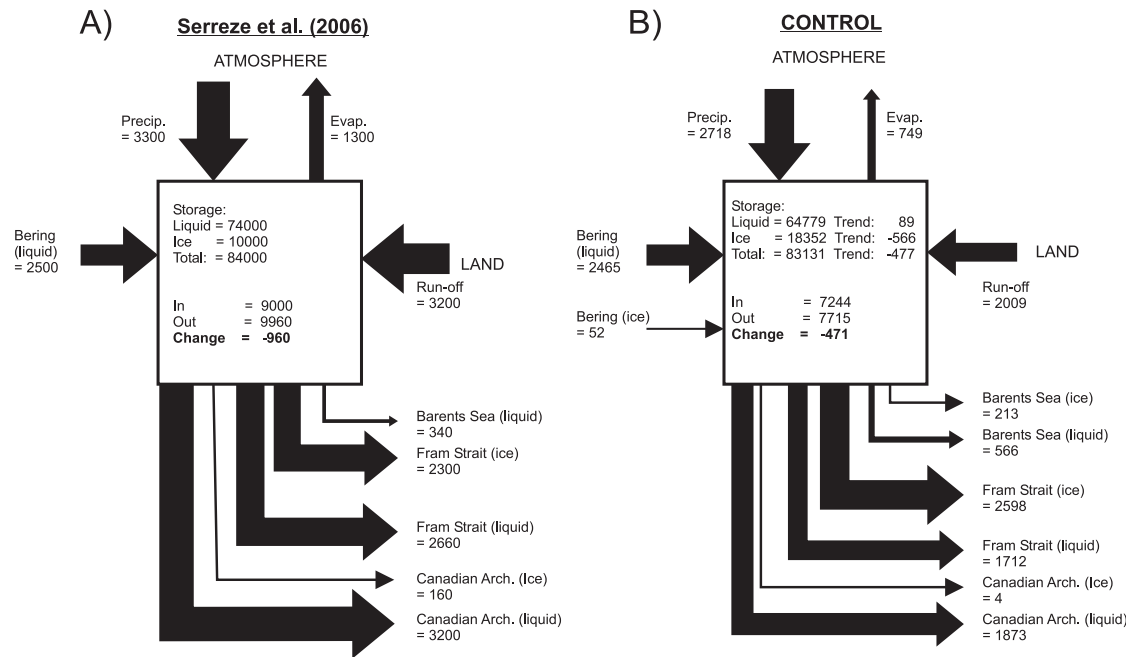


FIG. 3. Mean freshwater budget for the Arctic (a) based on observations from Serreze et al. (2006) and (b) calculated over the period 1992–2001 for the control integration. Unit for all fluxes and trends is  $\text{km}^3 \text{yr}^{-1}$  and for freshwater storage  $\text{km}^3$  (see text for additional information); widths of the arrows are proportional to the size of the transports.

freshwater sinks to the Arctic; the EGC exports freshwater south, and the WSC imports salty water north into the Arctic. Serreze et al. (2006) split their analysis of Fram Strait into the Norwegian Coastal Current and Fram Strait upper and deep water. To facilitate a direct comparison with our model fluxes we consider all three components to be part of the total water exchanged through Fram Strait, giving an average liquid freshwater export of  $2660 \text{ km}^3 \text{yr}^{-1}$ . The model value of  $1712 \text{ km}^3 \text{yr}^{-1}$  is  $\sim 64\%$  of the climatological value. The export of sea ice through Fram Strait has been fairly extensively examined (Vinje et al. 1998; Kwok et al. 2004), with the climatology value of  $2300 \text{ km}^3 \text{yr}^{-1}$  in good agreement with the  $2598 \text{ km}^3 \text{yr}^{-1}$  from the model.

Accurate measurements of the freshwater fluxes through the Canadian Archipelago are more difficult to make owing to the remoteness and large area covered by this complex network of channels, leading to a wide range of estimates in the literature from  $1700$  to  $3500 \text{ km}^3 \text{yr}^{-1}$ . Serreze et al. (2006) use the mean annual liquid freshwater discharge of  $3200 \text{ km}^3 \text{yr}^{-1}$  from Prinsenberg and Hamilton (2005), and their accompanying  $160 \text{ km}^3 \text{yr}^{-1}$  sea ice export estimate. These values are based upon three years of measurements across Lancaster Sound, combined with model results. Relative to the climatology, the model underestimates the export of both the liquid and sea ice freshwater components through the Canadian Archipelago, with values of  $1873$  and  $4 \text{ km}^3 \text{yr}^{-1}$ , respectively. We point out, however, that our modeled

TABLE 1. Freshwater transports ( $\text{km}^3 \text{yr}^{-1}$ ) in the climatology and the control integration, shown as the annual mean from the 10-yr integration. Negative values represent an export of freshwater from the Arctic.

	Fram Strait	Barents Sea	Bering Strait	Canadian Archipelago	$P - E$	Runoff
Liquid						
Observations	−2660	−340	2500	−3200	2000	3200
Control run	−1712	−566	2465	−1873	1969	2009
Difference	−948	226	35	−1327	31	1191
Ice						
Observations	−2300	0	0	−160		
Control run	−2598	−213	52	−4		
Difference	298	213	−52	−156		

freshwater export is close to the lower estimate of  $1700 \text{ km}^3 \text{ yr}^{-1}$  given in Serreze et al.

Overall, the largest discrepancies between the model and the observational estimates are due to the liquid freshwater export at Fram Strait (64%), the Canadian Archipelago (58%), and continental runoff (63%) (Table 1). Figure 3 shows the Arctic freshwater budget of Serreze et al. (2006) and the corresponding budget for the control run, based on the annual mean from 1992 to 2001. There is a slight imbalance in the control model budget of  $6 \text{ km}^3 \text{ yr}^{-1}$  resulting from the freshwater fluxes into the Arctic not quite balancing the changes in the calculated volume of freshwater in the Arctic. This is due to calculating the budget with monthly model output data. However, we note that the imbalance is very small—at least two orders of magnitude less than the major freshwater sources and sinks to the Arctic.

To a large degree the observed and modeled budgets are very similar, with the total estimated freshwater storage and exchanges in good agreement in both cases. Our control integration indicates that more freshwater ( $471 \text{ km}^3 \text{ yr}^{-1}$ ) leaves the Arctic than is received for the period 1992–2001, and a similar, although larger imbalance of  $960 \text{ km}^3 \text{ yr}^{-1}$  is also noted in the climatology. Although observational errors may play a part in this imbalance (Serreze et al. 2006), it likely indicates that the observations were biased to a period of net Arctic freshwater loss, as suggested by Peterson et al. (2006).

From year 0 to years 3 and 4 (corresponding to calendar years 1992 and the mid-1990s for the control integration only) there is an initial  $7000 \text{ km}^3$  decline in the total liquid and ice freshwater volume, in the control integration. This is then followed by a  $\sim 5000 \text{ km}^3$  recovery in total freshwater volume by the end of year 7 (Fig. 4). The change in the freshwater balance is very similar and of the same order of magnitude, as those observed in the previously discussed Arctic regional models of Köberle and Gerdes (2007) and Häkkinen and Proshutinsky (2004), and is a pattern similar to the large-scale changes observed in the NAO pattern during this period. To understand this link further we now investigate, in detail, the direct response of the Arctic freshwater budget to the different phases of the NAO.

#### 4. Response to persistent NAO forcing

##### a. Changes in the freshwater budget

Repeatedly forcing the regional model with NAO+ forcing reduces the total volume of freshwater stored in the Arctic by approximately  $1300 \text{ km}^3 \text{ yr}^{-1}$  (Fig. 5). After 10 years of integration time,  $13\,034 \text{ km}^3$  of freshwater have been lost from the Arctic system, equivalent

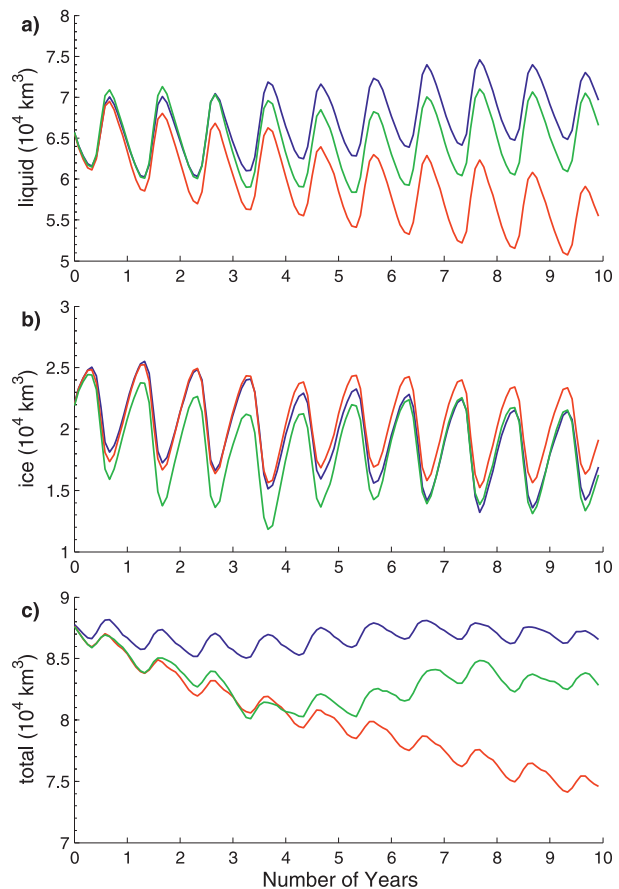


FIG. 4. Monthly storage in the Arctic of (a) liquid, (b) sea ice, and (c) total (liquid + sea ice) freshwater for the control (green line), NAO- (blue line), and NAO+ (red line) integrations.

to a 15% reduction in total freshwater storage, with three-quarters of this adjustment occurring in the liquid fraction (Fig. 4).

The loss of liquid freshwater occurs primarily in the Beaufort gyre, as shown by the significantly depleted pool of freshwater stored in this region at the end of the integration (lower-right panel in Fig. 6). The vertical thickness of freshwater in the gyre has reduced from a maximum of 20 m at the beginning of the integration to 17 m after 10 years (Fig. 6). At the same time, the edge of the CHL retreated east of its initial position on the Lomonosov Ridge (as marked by the strong boundary between relatively fresh and saline waters in Fig. 6) toward the Mendeleev Ridge. In the model, the retreat of the CHL is concurrent with an increase in the volume of warm, salty AW entering the Arctic from the Barents Sea and penetrating along the Siberian coast (not shown).

A loss of sea ice from the Arctic causes the volume of stored freshwater to be reduced by approximately  $2900 \text{ km}^3$  (13%) in 10 years. We find that sea ice primarily thinned in the central Arctic but thickened to the

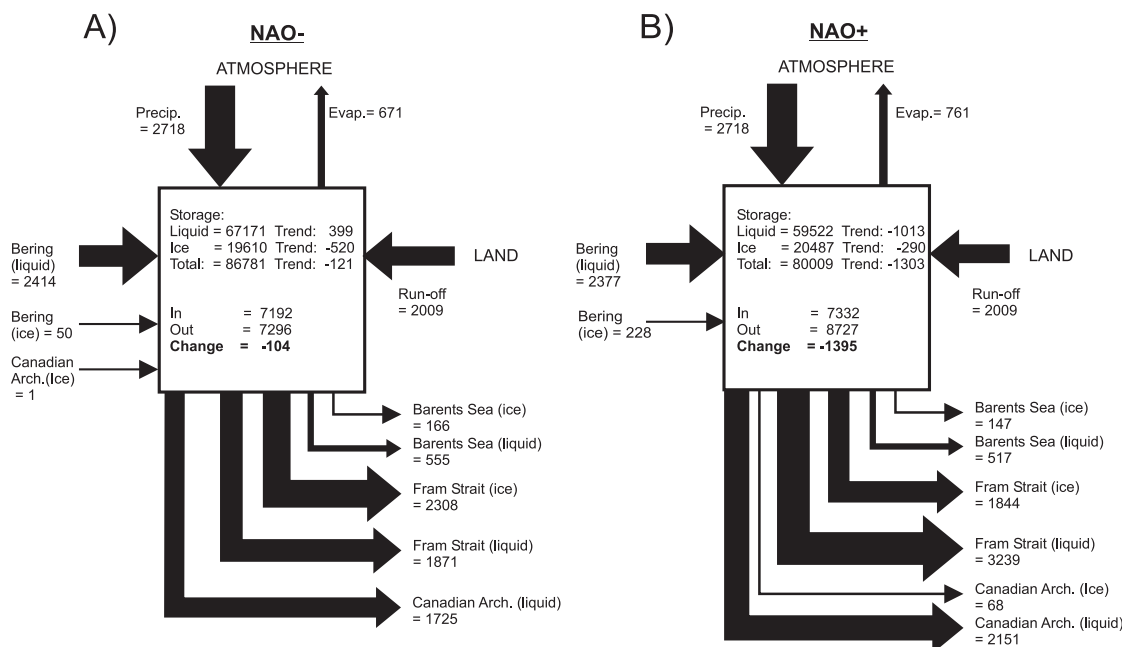


FIG. 5. Annual mean freshwater budget ( $\text{km}^3 \text{yr}^{-1}$ ) of the Arctic in response to (left) NAO– and (right) NAO+ forcing (shown as the annual mean for the 10-yr integrations) for all fluxes and trends and freshwater storage ( $\text{km}^3$ ); see text for additional information. The widths of the arrows are proportional to the size of the transports.

west along the north coast of Greenland and Ellesmere Island (not shown), as the prevailing winds cause the ice to concentrate in this region.

In contrast to the NAO+ integration, for NAO– forcing the Arctic retains virtually its entire storage of freshwater (Fig. 5). Remarkably, after 10 years of integration time, the total Arctic freshwater volume of  $86\,546 \text{ km}^3$  implies that only 1% of the initial freshwater storage has been lost from the system (Fig. 4). The freshwater pool in the Beaufort Sea remains largely intact, with a maximum vertical thickness of 18.5 m, while the edge of the CHL stays close to its initial position on the Lomonosov Ridge (lower-middle panel in Fig. 6). In short, there is very little drift in the freshwater distribution from the conditions used to initialize the model.

The decline in the total volume of freshwater stored in the Arctic during the NAO+ integration is largely a response to an increase in the export of freshwater to the North Atlantic via Fram Strait and the Canadian Archipelago (Table 2). During the NAO+ integration the total flux of freshwater through these straits was, on average,  $906$  and  $495 \text{ km}^3 \text{yr}^{-1}$  higher than the NAO– integration, respectively. The increase at Fram Strait is entirely due to an increase in sea ice export, and we find that the 43% increase in sea ice export compares very well with the 56% change noted in the modeling study of Zhang et al. (2003) examining the response of the

Arctic to the different phases of the NAO. Despite the export of sea ice increasing at Fram Strait during the NAO+ integration, the volume of liquid freshwater transport was lower at this time and arises because the volume of freshwater flowing northward into the Arctic in the WSC increased by  $24 \text{ km}^3 \text{yr}^{-1}$ .

The rate of evaporation over the Arctic increases for the NAO+ integration, compared to both the control and NAO– integrations, thereby acting as a larger freshwater sink. The higher rate of evaporation is due to an elevated latent heat flux at the air–sea boundary as a result of the higher wind speeds during the positive phase of the NAO. However, the  $90 \text{ km}^3 \text{yr}^{-1}$  increase in the rate of evaporation accounts for only 6% of the increased freshwater loss from the system each year, suggesting it plays a fairly minor role in the observed change in the freshwater budget of the Arctic.

#### b. Passive dye tracer

To visualize the export pathways of freshwater stored in the Arctic we added a passive tracer with 100% concentration in the upper 200 m of the freshwater pool in the Beaufort gyre, where the initial integrated vertical thickness of freshwater exceeded 16 m (see Fig. 7 for the initial distribution). After 10 years, the dye in the NAO– integration is confined largely to the Canadian Basin and Beaufort Sea, showing a pattern similar to the vertically integrated freshwater distribution in Fig. 6

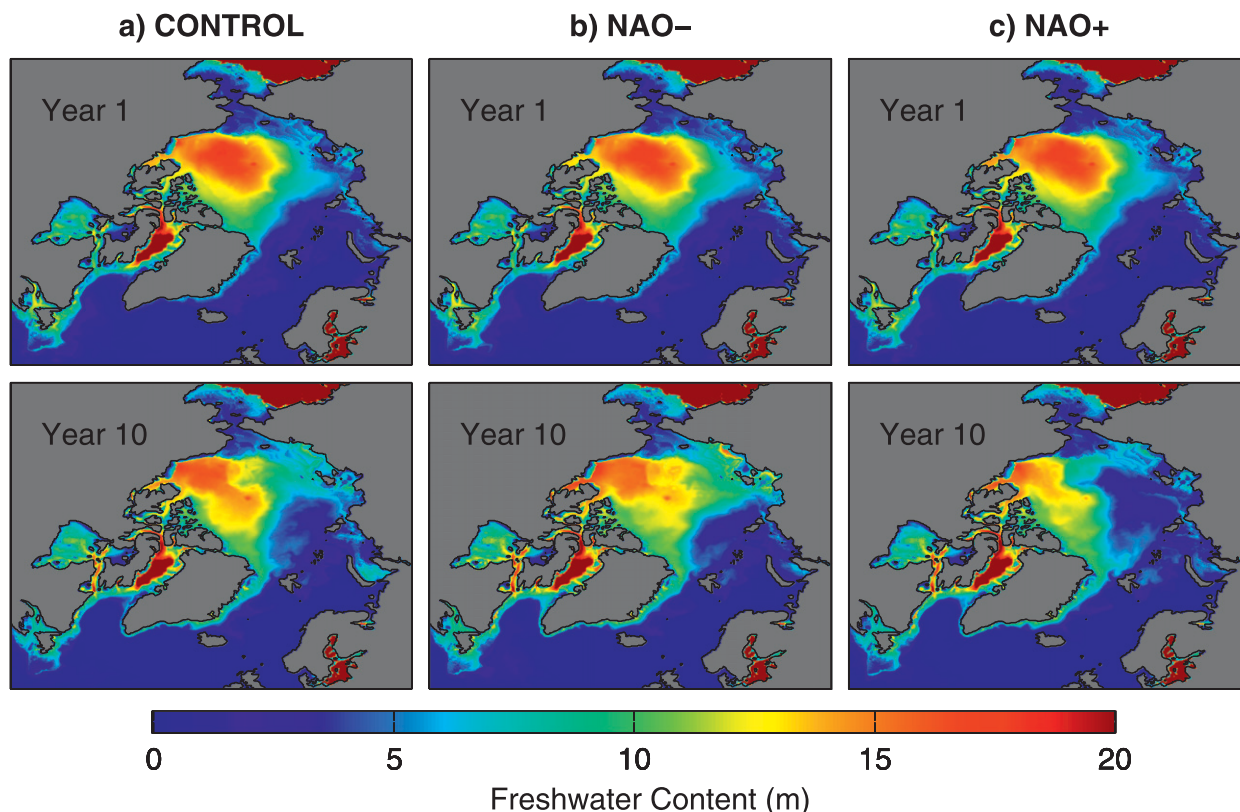


FIG. 6. Annual mean vertically integrated freshwater content (m) in the (a) control, (b) NAO–, and (c) NAO+ integrations for the first and last year of each simulation.

(Fig. 7a). The dye tracer is advected through the Canadian Archipelago as a coherent buoyant coastal current, flowing southward along the Baffin Island coast down to the Davis and Hudson Straits, and eventually along the Labrador coast. Low dye concentrations are also advected through Fram Strait, and we find that the dye has only made it to Denmark Strait at the end of the 10 yr integration.

In contrast, the dye in the NAO+ integration has been pushed farther westward toward the Queen Elizabeth Islands and the north coast of Greenland after 10 yr (Fig. 7b). The amount of dye advecting with the EGC is larger, passing around Cape Farewell and merging with the dye coming down Baffin Bay after 10 yr. In both integrations, the passive dye tracer is confined to the shelf break once it leaves the Arctic, with no evidence of offshore flow along the East Greenland coast, or along the Baffin and Labrador coasts in all integrations.

The different spatial patterns in the dye advecting through the Canadian Archipelago indicates that the pathway of exchange between the Arctic and the Labrador Sea through this complex region of islands and channels varies with the phase of the NAO. An analysis of the 10-yr annual mean freshwater transports indicates

that during the NAO+ integration a higher percentage (+5%) of the total Canadian Archipelago outflow of freshwater passes through Nares Strait, with a 7% reduction through the Amundsen Sea to the west. The changing spatial pattern is in agreement with the advection of the dye toward Ellesmere Island and the north coast of Greenland in the NAO+ integration. However, it is interesting that the relative percentage changes at each of the straits are small. The fraction of the total

TABLE 2. Annual mean freshwater transports ( $\text{km}^3 \text{yr}^{-1}$ ) for the two 10-yr NAO forcing experiments, separated into the liquid and ice fractions. Negative values represent an export of freshwater from the Arctic.

	Fram Strait	Barents Sea	Bering Strait	Canadian Archipelago	$P - E$
Liquid					
NAO+	–1844	–517	2377	–2151	1957
NAO–	–1871	–555	2414	–1725	2047
Difference	27	38	–37	–426	–90
Ice					
NAO+	–3239	–147	228	–68	
NAO–	–2308	–166	50	1	
Difference	–931	19	178	–69	

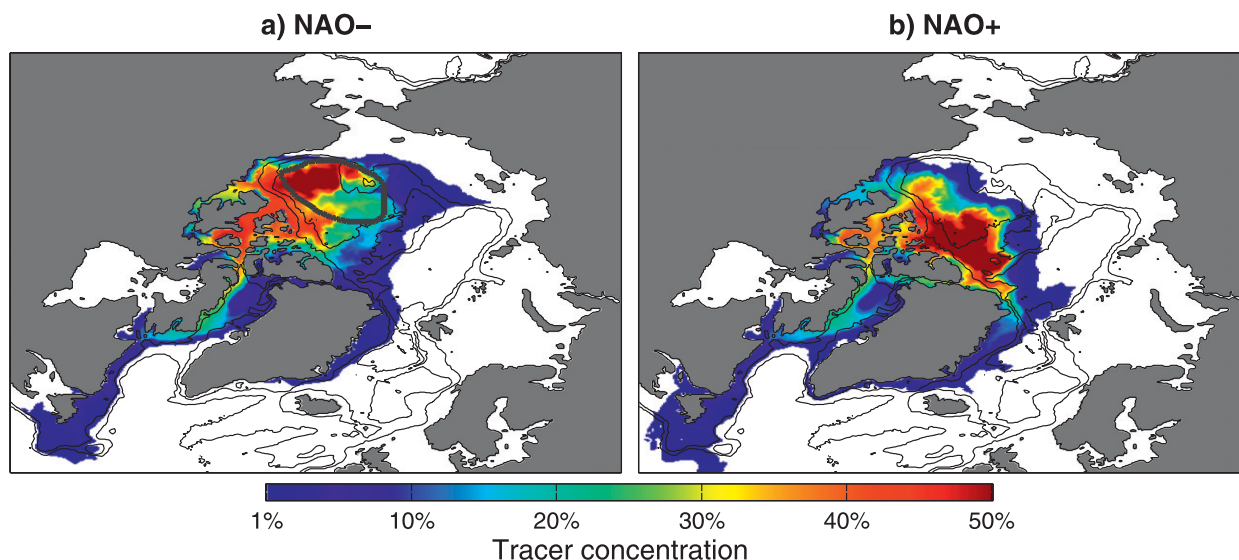


FIG. 7. Beaufort Sea tracer averaged over the upper 50 m of the water column for the final year (year 10) of each integration, showing concentrations greater than 1% for (a) NAO- and (b) NAO+. The dashed black line in the left panel shows the initial spatial distribution of the tracer that was added in the upper 200 m of the water column where the vertically integrated freshwater thickness initially exceeded 16 m. Bathymetry contours are 500 and 2500 m.

Canadian Archipelago freshwater flowing through the Queen Elizabeth Islands and M'Clure Strait remain virtually the same in both NAO+ and NAO- integrations; they only differ by 2%.

### c. Long-term evolution

The strong response in the storage of freshwater in the Arctic to persistent NAO forcing led us to consider the long-term evolution in the volume of freshwater stored in the Arctic. We initially consider what happens to the storage of freshwater in the Arctic if the positive phase of the NAO persists beyond 10 yr, and then investigate whether the freshwater content of the system can recover if the NAO switches back to its negative phase. To get a first-order idea about the systems response we performed a 30-yr-long NAO+ integration and a 20-yr NAO- integration, which starts from the conditions in the Arctic after 10 yr of NAO+ forcing.

The 30-yr NAO+ integration shows an exponential decay of freshwater volume, which seems to taper off toward a new equilibrium after 25–30 yr (Fig. 8), as the freshwater fluxes begin to balance. After 30 yr, the Arctic has a total freshwater volume of  $65\,130\text{ km}^3\text{ yr}^{-1}$ , implying that over a quarter of the original freshwater content of the system has been removed. The storage of freshwater in the Canadian Basin is virtually absent at this time, having been replaced by warm, salty Atlantic water, while the freshwater pool is largely confined to a small area of the Beaufort Sea, with a maximum freshwater thickness of 14 m (not shown). As the Arctic ap-

proaches what appears to be a new equilibrium, the average freshwater fluxes for the last 5 years of the integration indicate that the total export of freshwater to the North Atlantic via Fram Strait has now significantly weakened. In fact, the total export of  $4151\text{ km}^3\text{ yr}^{-1}$  is more typical of when the NAO was negative (see Table 2 as a reference). In contrast, we find that the export of freshwater through the Canadian Archipelago remains high with a southward transport of  $2291\text{ km}^3\text{ yr}^{-1}$  that is close to the 10-yr average for the NAO+ integration. To balance the persistent export of freshwater from the Arctic through the Canadian Archipelago, we find that the inflow of freshwater through Bering Strait increased to  $2771\text{ km}^3\text{ yr}^{-1}$ .

Our second long integration shows that the volume of liquid Arctic freshwater is able to recover almost completely in just 10 years (Fig. 8a) following a switch in the phase of the NAO (from positive to negative), with the liquid freshwater volume only 4% less than its initial value at this time. However, it takes 15–20 yr for the total freshwater volume (including sea ice) to recover close to its initial volume (Fig. 8b). Remarkably, after only 20 years of integration from the point in time when the NAO forcing switches, the total Arctic freshwater content recovers to within 1% of its initial value. Moreover, the pool of freshwater stored in the Beaufort gyre has reformed with a maximum vertical freshwater thickness of 18 m, while the edge of the CHL also lies very close to its initial position along the Lomonosov Ridge (not shown).

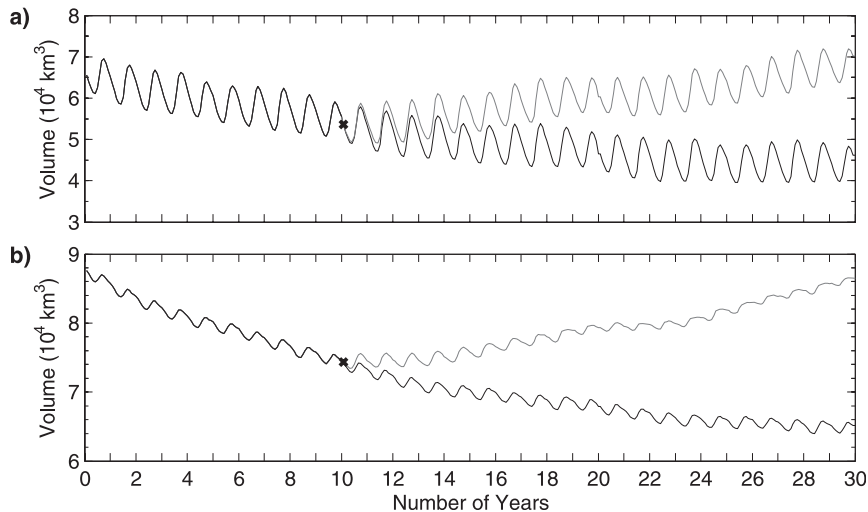


FIG. 8. Monthly mean freshwater volume of the Arctic from a 30-yr integration using NAO+ forcing (black line) and a second integration using NAO- forcing starting from the ocean state after 10 years of NAO+ forcing (gray line). The black cross ( $\times$ ) indicates the point at which the forcing was switched. The figure shows (a) the liquid freshwater volume and (b) the total freshwater volume (ice included). The freshwater volume in the continuous NAO+ run stabilizes after  $\sim 25$ – $30$  yr at a new equilibrium with a total freshwater  $\sim 65\,000\text{ km}^3$ .

## 5. Discussion and conclusions

Comparing the Arctic freshwater budget in our control integration to the most recent observational Arctic freshwater budget of Serreze et al. (2006) indicates that our regional model is able to represent the freshwater system of the Arctic Ocean with a high degree of realism.

The results from these two integrations show a dramatically different response in the freshwater budget of the Arctic to the positive and negative phases of the NAO that we have quantified in this study. A wind-forcing pattern typical of the positive phase of the NAO causes freshwater initially stored in the Arctic's Beaufort gyre to drain into the North Atlantic, primarily through Fram Strait and the Canadian Archipelago, while the negative phase of the NAO causes freshwater stored in this gyre to be almost entirely retained. In addition, our two long NAO integrations show that when the NAO remains positive for 30 yr the Arctic begins to reach a new, freshwater-depleted equilibrium but, if the NAO returns to its negative phase after a decade of positive activity, the model does not drift away but recovers its freshwater content almost entirely. We therefore suggest that the persistence of the NAO in a particular phase for a decade does not necessarily mean that the Arctic will cross a critical threshold beyond which it cannot return to its previous state. On the contrary, it suggests a more dynamic system that can exist in several freshwater states.

We note that the model results presented here, including the response to the NAO, are from a regional

ocean–ice model in which the fluxes at the sides and the air–sea boundary conditions are prescribed from a global model integration and atmospheric reanalysis data, respectively. Hence, they cannot respond and evolve with feedbacks associated with change in the regional ocean–ice model. Furthermore, with the exception of the wind velocity data, all of the remaining forcing variables are taken from the period 1992–2001 when the NAO was by and large positive, and an increasing number of midlatitude synoptic storms penetrated into the Arctic, increasing the northward moisture and heat transport (Zhang et al. 2004). During the period of NCEP forcing (1992–2001) the air temperature over the Arctic rose by approximately  $0.5^\circ\text{C}$ , in contrast to the 1960s (when the NAO was negative) when the air temperature was, on average, over  $1^\circ\text{C}$  colder (Shein et al. 2006). This warming trend likely accounts for the downward trend in sea ice content observed in all integrations (Fig. 4). However, by only modifying the wind field in our integrations it is straightforward to observe the variability in the Arctic freshwater budget associated with the positive and negative phase of the NAO.

Our results show that the changes in Arctic freshwater storage are strongly modulated by the expansion and contraction of the Beaufort gyre, as suggested by Proshutinsky and Johnson (1997), Proshutinsky et al. (2002), Zhang et al. (2003), Häkkinen and Proshutinsky (2004), and Peterson et al. (2006). During the positive phase of the NAO, the cyclonic atmospheric circulation reduces Ekman convergence in the Beaufort gyre and

allows freshwater stored in this region to escape as the gyre spins down. In contrast, during the negative phase of the NAO, the anticyclonic Beaufort high pressure over the central Arctic causes Ekman convergence and freshwater to be retained. The observed retention and reestablishment of the Beaufort gyre in our NAO—integrations toward a freshwater pattern very similar to the PHC data strongly suggests that we may be initializing our model with a dataset more representative of the Arctic during the negative phase of the NAO. Indeed, an examination of the period of data collection in this dataset confirms that observations were primarily taken during the winters of the 1970s (Timokhov and Tanis 1997), when the NAO was considerably more negative.

In agreement with the work of, for example, Curry and Mauritzen (2005) and Peterson et al. (2006), the increased export of freshwater to the North Atlantic when the NAO was positive in our model suggests that the observed freshening of the North Atlantic from the mid-1960s to the mid-1990s may have had its origin in the Arctic Ocean. This period of North Atlantic freshening coincides with a change in the NAO from its strongly negative to strongly positive state in which a weakening of the Beaufort high would reduce Ekman convergence in the gyre, leading to an increase in the export of stored freshwater to the North Atlantic. We find that the 30-yr observed trend toward an increasingly positive NAO matches the freshwater adjustment time scale of the Arctic in our model to repeat NAO+ wind forcing in our long NAO+ integration (Fig. 8). We also find that the increased export of  $1300 \text{ km}^3 \text{ yr}^{-1}$  of freshwater to the North Atlantic in our NAO+ integration is approximately two-thirds of the rate of increased export found for the 5-yr GSA event beginning in the late 1960s, examined by Dickson et al. (1988). Recent observations from Holliday et al. (2008) indicate that the freshening trend of the North Atlantic has reversed since the mid-1990s. This reversal comes at a time when the NAO became more neutral, suggesting that the reestablishment of the Beaufort gyre caused less freshwater to leak into the North Atlantic, compared to that in previous decades.

We have not, however, considered the direct effect of the NAO on the circulation of the North Atlantic subtropical and subpolar gyres, both of which have recently both been shown to directly affect the salinity and temperature of the North Atlantic (see, e.g., Hátún et al. 2005; Häkkinen and Rhines 2004). The changes observed in the freshwater content of the North Atlantic over the last 50 years are therefore very likely to have been influenced by freshwater export from the Arctic—also the strength of the subtropical and subpolar gyres—farther south.

The observed movement in the position of the CHL toward the western Arctic in our NAO+ integration is concurrent with the changes in freshwater content and is in good agreement with the work of Steele and Boyd (1998), supporting their hypothesis that the persistent positive state of the NAO during the early 1990s caused the CHL to retreat toward the Makarov Basin. Furthermore, our finding that negative NAO forcing caused the CHL to readvance toward its original position supports the observed return of the CHL to the Amundsen Basin in 2001 (Björk et al. 2002), following a period in the late 1990s and early 2000s when the NAO was more neutral in state.

The large increase in freshwater export observed through the Canadian Archipelago in our model during the NAO+ integration clearly illustrates the importance of resolving this gateway between the Arctic and sub-Arctic seas. In coarser-resolution models the complex network of islands and channels in this region are poorly represented (if at all). However, having an accurate representation of these straits has been shown to play an important role in obtaining a realistic strength for the MOC in a climate model, as it controls the fraction of freshwater exported either directly into the Nordic or Labrador Seas where it plays a role in modulating deep convective overturning (Wadley and Bigg 2002). Our finding that the flow through the Canadian Archipelago remained high as the model began to equilibrate after 30 yr of NAO+ forcing reiterates the need to resolve this region in order to accurately model the transport of freshwater from the Arctic to the sub-Arctic seas.

It is interesting that when resolving the shelves, shelf breaks, and associated buoyant coastal flow of freshwater in the Arctic with a model that has horizontal grid spacing of 18 km, there is little offshore advection of this buoyant coastal flow into either the central Labrador Sea or Nordic seas, where classical open ocean convection is thought to occur. Our results therefore suggest that a degree of caution should be used when interpreting the role of Arctic freshwater on the rates of deep convection. Indeed, in coarser-resolution models, broad diffuse currents from the Arctic cause Arctic freshwater to spread over the interior of these regions, much akin to freshwater-hosing experiments, where it can “cap” deep convection. In reality, instabilities along the shelf break and eddy mixing play a significant role in this process (Myers 2005).

The dye tracer shows that there is considerable interaction in our model between Arctic freshwater in the Labrador Current and the Gulf Stream at the tail of the Grand Banks. Indeed, how freshwater from the Arctic mixes with the Gulf Stream in this region, in terms of recirculation, movement southward along the continental

shelf, or supplementation of the deep western boundary current is a particularly interesting and largely unresolved area of study. At present, the close proximity of our open boundary conditions prescribed from our global calculation likely play a large role in controlling this interaction, making it difficult to interpret the results in this area.

## REFERENCES

- Aagaard, K., and E. C. Carmack, 1989: The role of sea ice and other fresh water in the Arctic circulation. *J. Geophys. Res.*, **94** (C10), 14 485–14 498.
- Adcroft, A., C. Hill, and J. Marshall, 1997: Representation of topography by shaved cells in a height coordinate ocean model. *Mon. Wea. Rev.*, **125**, 2293–2315.
- , J. M. Campin, C. Hill, and J. Marshall, 2004: Implementation of an atmosphere–ocean general circulation model on the expanded spherical cube. *Mon. Wea. Rev.*, **132**, 2845–2863.
- Arakawa, A., and V. Lamb, 1977: Computational design of the basic dynamical processes of the UCLA general circulation model. *Methods in Computational Physics: Advances in Research and Applications*, J. Chang, Ed., Academic Press, 173–265.
- Belkin, I. M., 2004: Propagation of the “Great Salinity Anomaly” of the 1990s around the northern North Atlantic. *Geophys. Res. Lett.*, **31**, L08306, doi:10.1029/2003GL019334.
- , S. Levitus, J. Antonov, and S. A. Malmberg, 1998: “Great Salinity Anomalies” in the North Atlantic. *Prog. Oceanogr.*, **41**, 1–68.
- Björk, G., J. Söderkvist, P. Winsor, A. Nikolopoulos, and M. Steele, 2002: Return of the cold halocline layer to the Amundsen Basin of the Arctic Ocean: Implications for the sea ice mass balance. *Geophys. Res. Lett.*, **29**, 1513, doi:10.1029/2001GL014157.
- Bryan, K., and L. J. Lewis, 1979: A water mass model of the world ocean. *J. Geophys. Res.*, **84**, 2503–2517.
- Curry, R., and C. Mauritzen, 2005: Dilution of the northern North Atlantic Ocean in recent decades. *Science*, **308**, 1772–1774.
- Daru, V., and C. Tenaud, 2004: High order one-step monotonicity-preserving schemes for unsteady compressible flow calculations. *J. Comput. Phys.*, **193**, 563–594.
- Deser, C., 2000: On the teleconnectivity of the “Arctic Oscillation.” *Geophys. Res. Lett.*, **27**, 779–782.
- Dickson, R. R., J. Meincke, S.-A. Malmberg, and A. J. Lee, 1988: The great salinity anomaly in the Northern North Atlantic 1968–1982. *Prog. Oceanogr.*, **20**, 103–151.
- , and Coauthors, 2000: The Arctic Ocean response to the North Atlantic Oscillation. *J. Climate*, **13**, 2671–2696.
- Gent, P. R., and J. C. McWilliams, 1990: Isopycnal mixing in ocean circulation models. *J. Phys. Oceanogr.*, **20**, 150–155.
- Haak, H., J. Jungclaus, U. Mikolajewicz, and M. Latif, 2003: Formation and propagation of great salinity anomalies. *Geophys. Res. Lett.*, **30**, 1473, doi:10.1029/2003GL017065.
- Häkkinen, S., and A. Proshutinsky, 2004: Freshwater content variability in the Arctic Ocean. *J. Geophys. Res.*, **109**, C03051, doi:10.1029/2003JC001940.
- , and P. B. Rhines, 2004: Decline of subpolar North Atlantic circulation during the 1990s. *Science*, **304**, 555–559.
- Hátún, H., A. B. Sandø, H. Drange, B. Hansen, and H. Valdimarsson, 2005: Influence of the Atlantic subpolar gyre on the thermohaline circulation. *Science*, **309**, 1841–1844.
- Hibler, W. D., III, 1979: A dynamic thermodynamic sea ice model. *J. Phys. Oceanogr.*, **9**, 815–846.
- , and K. Bryan, 1987: A diagnostic ice–ocean model. *J. Phys. Oceanogr.*, **17**, 987–1015.
- Holliday, N. P., and Coauthors, 2008: Reversal of the 1960s to 1990s freshening trend in the northeast North Atlantic and Nordic Seas. *Geophys. Res. Lett.*, **35**, L03614, doi:10.1029/2007GL032675.
- Houssais, M. N., C. Herbaut, P. Schlichtholz, and C. Rousset, 2007: Arctic salinity anomalies and their link to the North Atlantic during a positive phase of the Arctic Oscillation. *Prog. Oceanogr.*, **73**, 160–189.
- Hurrell, J. W., 1995: Decadal trends in the North Atlantic Oscillation: Regional temperatures and precipitation. *Science*, **269**, 676–679.
- Jackett, D. R., and T. J. McDougall, 1995: Minimal adjustment of hydrographic profiles to achieve static stability. *J. Atmos. Oceanic Technol.*, **12**, 381–389.
- Kalnay, E., and Coauthors, 1996: The NCEP/NCAR 40-Year Reanalysis Project. *Bull. Amer. Meteor. Soc.*, **77**, 437–471.
- Karcher, M., R. Gerdes, F. Kauker, C. Köberle, and I. Yashayaev, 2005: Arctic Ocean change heralds North Atlantic freshening. *Geophys. Res. Lett.*, **32**, L21606, doi:10.1029/2005GL023861.
- Köberle, C., and R. Gerdes, 2007: Simulated variability of the Arctic Ocean freshwater balance 1948–2001. *J. Phys. Oceanogr.*, **37**, 1628–1644.
- Kwok, R., G. F. Cunningham, and S. S. Pang, 2004: Fram Strait sea ice outflow. *J. Geophys. Res.*, **109**, C01009, doi:10.1029/2003JC001785.
- Lammers, R. B., A. I. Shiklomanov, C. J. Vorosmarty, B. M. Fekete, and B. J. Peterson, 2001: Assessment of contemporary Arctic river runoff based on observational discharge records. *J. Geophys. Res.*, **106** (D4), 3321–3334.
- Large, W. G., and S. Pond, 1981: Open ocean momentum flux measurements in moderate to strong winds. *J. Phys. Oceanogr.*, **11**, 324–336.
- , J. C. McWilliams, and S. C. Doney, 1994: Oceanic vertical mixing: A review and a model with a nonlocal boundary-layer parameterization. *Rev. Geophys.*, **32**, 363–403.
- Lazier, J. R. N., 1980: Oceanographic conditions at Ocean Weather Ship Bravo, 1964–1974. *Atmos.–Ocean*, **18**, 227–238.
- Leith, C. E., 1969: Diffusion approximation for two-dimensional turbulence. *Phys. Fluids*, **11**, 671–672.
- Manabe, S., and R. J. Stouffer, 1988: Two stable equilibria of a coupled ocean–atmosphere model. *J. Climate*, **1**, 841–866.
- Marshall, J., C. Hill, L. Perelman, and A. Adcroft, 1997: Hydrostatic, quasi-hydrostatic, and nonhydrostatic ocean modeling. *J. Geophys. Res.*, **102** (C3), 5733–5752.
- Maslowski, W., B. Newton, P. Schlosser, A. Semtner, and D. Martinson, 2000: Modeling recent climate variability in the Arctic Ocean. *Geophys. Res. Lett.*, **27**, 3743–3746.
- Menemenlis, D., and Coauthors, 2005: NASA supercomputer improves prospects for ocean climate research. *Eos, Trans. Amer. Geophys. Union*, **86**, doi:10.1029/2005EO090002.
- Morison, J., K. Aagaard, and M. Steele, 2000: Recent environmental changes in the Arctic: A review. *Arctic*, **53**, 359–371.
- Myers, P. G., 2005: Impact of freshwater from the Canadian Arctic Archipelago on Labrador Sea Water formation. *Geophys. Res. Lett.*, **32**, L06605, doi:10.1029/2004GL022082.
- Mysak, L. A., K. M. Wright, J. Sedláček, and M. Eby, 2005: Simulation of sea ice and ocean variability in the Arctic during 1955–2002 with an intermediate complexity model. *Atmos.–Ocean*, **43**, 101–118.

- Parkinson, C. L., and W. M. Washington, 1979: A large-scale numerical model of sea ice. *J. Geophys. Res.*, **84**, 311–337.
- Peterson, B. J., J. McClelland, R. Curry, R. M. Holmes, J. E. Walsh, and K. Aagaard, 2006: Trajectory shifts in the Arctic and subarctic freshwater cycle. *Science*, **313**, 1061–1066.
- Polyakov, I. V., and Coauthors, 2005: One more step toward a warmer Arctic. *Geophys. Res. Lett.*, **32**, L17605, doi:10.1029/2005GL023740.
- Prinsenberg, S. J., and J. Hamilton, 2005: Monitoring the volume, freshwater and heat fluxes passing through Lancaster Sound in the Canadian Arctic Archipelago. *Atmos.–Ocean*, **43**, 1–22.
- Proshutinsky, A. Y., and M. A. Johnson, 1997: Two circulation regimes of the wind-driven Arctic Ocean. *J. Geophys. Res.*, **102** (C6), 12 493–12 514.
- , R. H. Bourke, and F. A. McLaughlin, 2002: The role of the Beaufort Gyre in Arctic climate variability: Seasonal to decadal climate scales. *Geophys. Res. Lett.*, **29**, 2100, doi:10.1029/2002GL015847.
- Quadfasel, D., A. Sy, D. Wells, and A. Tunik, 1991: Warming in the Arctic. *Nature*, **350**, 385.
- Rahmstorf, S., 1995: Bifurcations of the Atlantic thermohaline circulation in response to changes in the hydrological cycle. *Nature*, **378**, 145–149.
- , and Coauthors, 2005: Thermohaline circulation hysteresis: A model intercomparison. *Geophys. Res. Lett.*, **32**, L23605, doi:10.1029/2005GL023655.
- Redi, M. H., 1982: Oceanic isopycnal mixing by coordinate rotation. *J. Phys. Oceanogr.*, **12**, 1154–1158.
- Semtner, A. J., 1976: A model for the thermodynamic growth of sea ice in numerical investigations of climate. *J. Phys. Oceanogr.*, **6**, 379–389.
- Serreze, M. C., and Coauthors, 2006: The large-scale freshwater cycle of the Arctic. *J. Geophys. Res.*, **111**, C11010, doi:10.1029/2005JC003424.
- Shein, K. A., and Coauthors, 2006: State of the climate in 2005. *Bull. Amer. Meteor. Soc.*, **87**, S6–S102.
- Steele, M., and T. Boyd, 1998: Retreat of the cold halocline layer in the Arctic Ocean. *J. Geophys. Res.*, **103** (C5), 10 419–10 435.
- , R. Morley, and W. Ermold, 2001: PHC: A global ocean hydrography with a high-quality Arctic Ocean. *J. Climate*, **14**, 2079–2087.
- Stephenson, D. B., V. Pavan, M. Collins, M. M. Junge, and R. Quadrelli, 2006: North Atlantic Oscillation response to transient greenhouse gas forcing and the impact on European winter climate: A CMIP2 multi-model assessment. *Climate Dyn.*, **27**, 401–420.
- Stouffer, R. J., and Coauthors, 2006: Investigating the causes of the response of the thermohaline circulation to past and future climate changes. *J. Climate*, **19**, 1365–1387.
- Sundby, S., and K. Drinkwater, 2007: On the mechanisms behind salinity anomaly signals of the northern North Atlantic. *Prog. Oceanogr.*, **73**, 190–202.
- Thompson, D. W. J., and J. M. Wallace, 1998: The Arctic Oscillation signature in the wintertime geopotential height and temperature fields. *Geophys. Res. Lett.*, **25**, 1297–1300.
- Timokhov, L., and F. Tanis, 1997: *Environmental Working Group Joint U.S.-Russian Atlas of the Arctic Ocean—Winter Period*. Environmental Research Institute of Michigan, National Snow and Ice Data Center, CD-ROM. [Available online at <http://nsidc.org/data/g01961.html>.]
- Vinje, T., N. Nordlund, and A. Kvambekk, 1998: Monitoring ice thickness in Fram Strait. *J. Geophys. Res.*, **103** (C5), 10 437–10 449.
- Wadley, M. R., and G. R. Bigg, 2002: Impact of flow through the Canadian Archipelago and Bering Strait on the North Atlantic and Arctic circulation: An ocean modelling study. *Quart. J. Roy. Meteor. Soc.*, **128**, 2187–2203.
- Zhang, J., and W. D. Hibler III, 1997: On an efficient numerical method for modeling sea ice dynamics. *J. Geophys. Res.*, **102** (C4), 8691–8702.
- , and D. A. Rothrock, 2003: Modeling global sea ice with a thickness and enthalpy distribution model in generalized curvilinear coordinates. *Mon. Wea. Rev.*, **131**, 845–861.
- , W. D. Hibler III, M. Steele, and D. A. Rothrock, 1998a: Arctic ice–ocean modeling with and without climate restoring. *J. Phys. Oceanogr.*, **28**, 191–217.
- , D. A. Rothrock, and M. Steele, 1998b: Warming of the Arctic Ocean by a strengthened Atlantic inflow: Model results. *Geophys. Res. Lett.*, **25**, 1745–1748.
- Zhang, R., and G. K. Vallis, 2006: Impact of great salinity anomalies on the low-frequency variability of the North Atlantic climate. *J. Climate*, **19**, 470–482.
- Zhang, X., M. Ikeda, and J. E. Walsh, 2003: Arctic sea ice and freshwater changes driven by the atmospheric leading mode in a coupled sea ice–ocean model. *J. Climate*, **16**, 2159–2177.
- , J. E. Walsh, J. Zhang, U. S. Bhatt, and M. Ikeda, 2004: Climatology and interannual variability of Arctic cyclone activity: 1948–2002. *J. Climate*, **17**, 2300–2317.